

Chapter Ten

Moist dynamics of tropical convection zones in monsoons, teleconnections and global warming

J. David Neelin

10.1 INTRODUCTION

10.1.1 Approach

In tropical dynamics, a leading feature is the interaction of the large-scale circulation with moist processes arising at small scales. This chapter summarizes a recent avenue of tropical theory for this interaction, in which constraints from the moist dynamics can actually simplify large-scale theory under certain conditions. Important tools in this approach include convective quasi-equilibrium (QE) and the moist static energy (MSE) budget. Convective QE (Arakawa and Schubert 1974; Emanuel et al. 1994) is the postulate, used in various forms in a number of convective parameterizations, that moist convection tends to alter the large-scale temperature and moisture vertical profiles in a manner that reduces the buoyancy available to small-scale overturning motions. A further summary of QE may be found in Chapter 7 in this volume. The aspects required here are the tendency of moist convection to constrain the temperature profile and to establish a relationship between temperature and moisture.

In outlining the approach to moist dynamics advocated here, three applications are considered—monsoons, tropical teleconnections and tropical precipitation changes under global warming. Background for these is provided in the remainder of this section, aiming also to convey the challenges of analysing large-scale flow interacting with moist convection. With this motivation, section 10.2 outlines the moist static energy budget and a useful quantity that arises from it under QE approximations, the gross moist stability. A numerical model, the Quasi-equilibrium Tropical Circulation Model (QTCM), whose formulation has been designed to mesh with this theoretical framework is sketched in section 10.3. This model is used in simulating the phenomena considered, but its particular value is the relative simplicity of analysis—either in pointing to solution features to analyse in observations or more complex models, or generating simpler models from its equations.

A consequence of viewing the thermodynamics via the moist static energy budget is the importance of the net flux into the atmospheric column and implications for land-sea contrast, as outlined in section 10.4. This ties directly to the first appli-

cation, mechanisms setting monsoon poleward boundaries, in section 10.5. Theory for how precipitation anomalies arise in these moist dynamical interactions, along with treatment of cloud feedbacks and land versus ocean cases in this framework, is summarized in sections 10.6 and 10.7. How such diagnostics apply to moist teleconnection theory (section 10.9), and tropical precipitation anomalies under global warming (section 10.10) is then addressed.

We know there are limits of validity to the approximations used here, particularly as one moves to the small scales. The boundaries of the regime of validity have not yet been well determined and this is part of the current direction of this research area. Statements of where limitations or modifications are believed by this author (in discussion with several colleagues noted in the acknowledgments) to be likely to arise are included in the form of postulates, denoted *Open question:* or *Postulate* as appropriate. The hope is to summarize phenomena and scales where this particular approach shows promise, while tempting the reader with aspects that are as yet unresolved.

10.1.2 Monsoon background

There is a rich literature on various monsoon systems: Asian (Ramage 1971; Riehl 1979; Luo and Yanai 1984; Murakami 1987; Ding 1992; Yasunari and Seki 1992; Ding 1994; Lau and Yang 1996; Li and Yanai 1996; Webster et al. 1998; Annamalai et al. 1999 and references therein), North American (e.g., Douglas et al. 1993; Higgins et al. 1997; Barlow et al. 1998; Yu and Wallace 2000), African (e.g., Palmer 1986; Xue and Shukla 1993; Lare and Nicholson 1994; Rowell et al. 1995; Eltahir and Gong 1996; Cook 1997; Semazzi and Sun 1997; Janicot et al. 1998) and South American (e.g., Lenters and Cook 1997; Zhou and Lau 1998, Nogues-Paegle et al. 2002). It is not possible here to review this vast body of work [see, e.g., Webster (1987); Young (1987) for an introduction]. Rather the aim here is to add a particular moist dynamical perspective on the large-scale aspects of these systems. Chapter 9 in this volume provides a complementary perspective on monsoon dynamics.

The term monsoon has migrated from older definitions (Ramage 1971) to recent usage emphasizing regions with “pronounced summertime precipitation maxima” (Yu and Wallace 2000), sometimes including ocean regions adjacent to continental monsoon regions (Chao 2000). Many aspects of the circulation such as an upper level anti-cyclone, and energetics commonly associated with monsoons (Webster 1987; Douglas et al. 1993; Zhou and Lau 1998) are intimately linked to this large scale seasonal movement of the tropical convergence zones.

For reference, and to illustrate issues that arise in a precipitation-centred view of the monsoons, Fig. 10.1 shows climatological rainfall (from the Xie and Arkin (1997) data set, 1979-1998 average) for Dec.-Feb. (DJF) and June-Aug. (JJA), processed in two ways. First, as a percent of annual rainfall; second, as the seasonal excess relative to the annual mean. Both are measures of the monsoon characteristic of high summer rainfall relative to the annual mean. From Fig. 10.1a,b, a fraction of 40% of annual occurring in JJA would be a plausible monsoon indicator (50% would exclude some traditional monsoon regions). But by this measure,

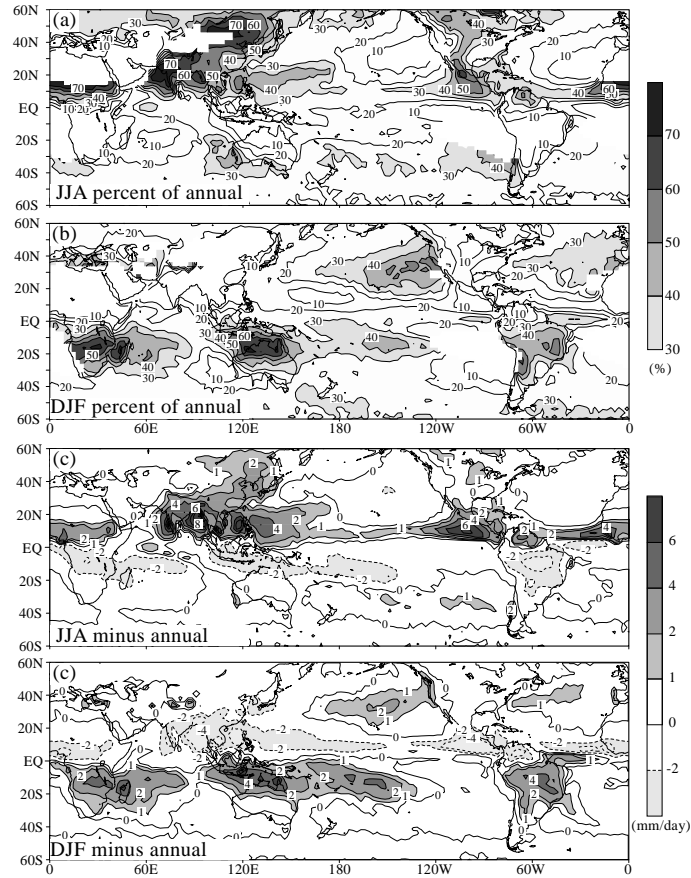


Figure 10.1 Observed climatological rainfall for JJA and DJF, respectively, displayed as (a) and (b) seasonal rainfall as a percent of annual rainfall (contour interval ten percent, masked blank where annual rainfall less than 0.5 mm/day); (c) and (d) seasonal rainfall minus the annual mean (mm/day).

monsoon regions would extend far poleward in continental interiors in the summer hemisphere. Discussing the “Canadian Prairie monsoon” or the “Siberian monsoon” might be stretching the terminology, although by this measure they clearly exceed the “Arizona monsoon”. To have an impact on the circulation, the monsoon deep convective diabatic heating should be sufficiently large. From this point of view, Fig. 10.1c,d provides a better measure. A threshold as simple as 2 mm/day summer season precipitation excess (above the annual average) yields regions that correspond fairly well to current notions of the large scale monsoons. For the poleward boundary, the 2 mm/day precipitation contour lies fairly close to this in most locations, and this will be used later in model evaluation.

In terms of what maintains summer monsoons, land-ocean contrast has long been considered fundamental (Webster 1987; Young 1987). One might conjecture that the thermodynamics of ocean-atmosphere-land interaction could be the controlling factor in the forcing of monsoons. However, examining the relation between solar

heating of the continent and the associated monsoon rainfall, the rain zone does not extend as far poleward as the maximum heating would seem to indicate. This suggests that other mechanisms besides the land-sea heating contrast determine northward extent of summer monsoon. Many studies (Lofgren 1995; Meehl 1994a,b; Xue and Shukla 1993; Yang and Lau 1998; Nicholson 2000) discuss the importance of land processes, such as soil moisture and surface albedo, in affecting the magnitude and position of the monsoon. Topography, such as the Tibetan Plateau, also affects the monsoon circulation (Flohn 1957; Murakami 1987; Meehl 1992; Yanai and Li 1994; Wu and Zhang 1998). The approach presented here follows Chou et al. (2001), Chou and Neelin (2001; 2003, CN03 hereafter) in showing how the land-sea contrast can be viewed in terms of the moist static energy budget and how large-scale dynamical mechanisms can mediate land-sea contrast to determine the poleward extent of the monsoon.

10.1.3 Moist teleconnection/tropical precipitation in global warming background

To motivate development of theory for precipitation changes in tropical teleconnections and global warming, Fig. 10.2 shows a composite ENSO precipitation pattern from observations and three models forced by observed SST. Two are general circulation models (GCMs) used in numerical weather prediction from the European Centre for Medium-Range Weather Forecasts (ECMWF) and the National Center for Environmental Prediction (NCEP), and one is the intermediate complexity climate model, QTCM, summarized in section 10.3. The composite is for warm events (average of 1982-83, 1986-87, 1991-92, 1994-95) minus cold events (average of 1983-84, 1988-89, 1995-96).

Without belaboring the obvious, there is no way to construe the comparison of the GCM response to observations in Fig. 10.2 as satisfactory. This poor simulation occurs despite the fact that these are well respected models on which the most widely used reanalysis data sets are based. The point this underlines is that the simulation of teleconnected precipitation anomalies is a very challenging problem. This difficulty not only motivates the effort to understand the physical processes, but the sensitivity appears consistent with the several mechanisms that are argued to be responsible for such precipitation anomalies in section 10.9, building on the theory from previous sections.

Regarding the simulation by the QTCM in Fig. 10.2d, the agreement with observations is qualitative in terms of the region of negative anomalies, although the magnitude is reasonable. The negative anomalies over equatorial South America occur along the margin of the model simulated climatology of the convection zone, which is shifted with respect to observed. The fact that the intermediate complexity model fares slightly better than the GCMs in Fig. 10.2b,c likely has to do with the fact that ENSO precipitation anomalies were examined among other factors, such as simulation of the climatology, during model development and revision (Zeng et al. 2000, Su et al. 2001) since the model was designed with teleconnection theory in mind. The simulation makes it plausible that mechanisms diagnosed from the QTCM make a reasonable starting point, subject to suitable caveats, for taking apart the complex processes of moist teleconnections.

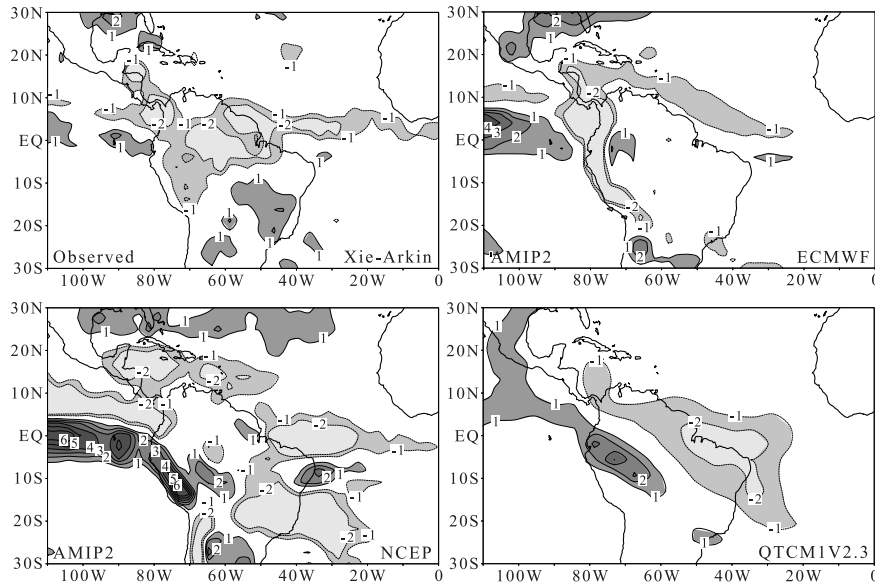


Figure 10.2 Composite precipitation anomaly (mm/day) for ENSO events during DJF. (a) Observed (Xie-Arkin data set) and three models forced by observed SST (no data assimilation). (b) ECMWF model; (c) NCEP model; (d) QTCM v2.3. ECMWF and NCEP data sets are from the Atmospheric Model Intercomparison project (AMIP2).

Figure 10.3 is a schematic based on analysis of the QTCM that was used in a series of talks trying to promote interest in moist teleconnection mechanisms during QTCM development in the late 1990s. One natural reaction to the diagram is that it appears complex. The processes, including the spreading of the warming by wave dynamics, the interaction of this with convection through QE considerations, cloud-radiative feedbacks and the role of mean flow acting on gradients of temperature and moisture, are consistent with present understanding which section 10.9 attempts to summarize. These processes roughly form the basis of such studies as Chiang and Sobel (2002), Su and Neelin (2002), Neelin et al. (2003, NCS03 hereafter) Neelin and Su (2005, NS05 hereafter), Chiang and Lintner (2005), Lintner and Chiang (2005). which have helped to systematize and somewhat condense the processes. Nonetheless, the fact remains that even in intermediate complexity models there is a fairly complex set of processes that can occur in moist teleconnections. This helps to explain the GCM difficulties in capturing these noted in Fig. 10.2, and raises the hope that improved understanding will help guide improved simulation.

In global warming simulations, large tropical precipitation changes occur (e.g. Boer et al. 2000b; Hu et al. 2000; Dai et al. 2001; Douville et al. 2002; Meehl et al. 2000; Roeckner et al. 1999; Yonetani and Gordon 2001; Williams et al. 2001; Allen and Ingram 2002; Johns et al. 2003; Manabe et al. 2004), including regions of substantial negative anomalies. The agreement on the regional distri-

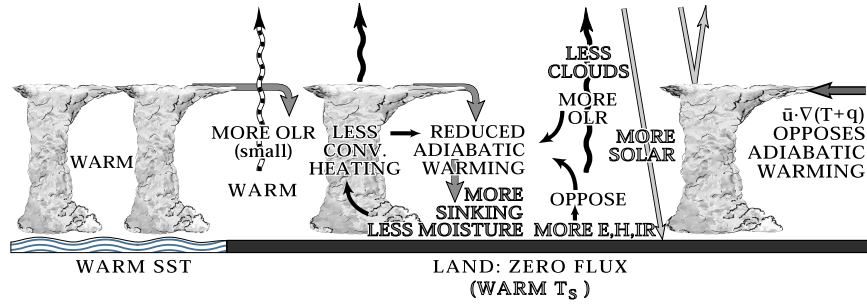


Figure 10.3 Schematic of the mechanisms at work in moist teleconnections including wave dynamics spreading tropospheric warming, interacting with convection and lower tropospheric moisture, cloud radiative feedbacks, land feedbacks, and climatological mean flow acting on the induced moisture and temperature gradients, as postulated in 1998.

bution of these is poor (Houghton et al. 2001; NCS03), akin to the agreement between models seen in the ENSO case in Fig. 10.2. Model evidence that a subset of the mechanisms at work in ENSO teleconnections creates the anomalies in global warming simulations is reviewed in section 10.10.

10.2 MOIST STATIC ENERGY ANALYSIS AND GROSS MOIST STABILITY

The moist static energy equation (section 10.2.1) sidesteps some of the large but cancelling terms that occur in the individual moisture and temperature equations. One can then exploit the tendency of convective QE to constrain temperature vertical structure through a deep convective layer, and to tie together moisture and temperature equations (section 10.2.5). If temperature and moisture in a column are not independent variables due to the QE constraints, then the moist static energy budget can determine the thermodynamics at leading order, under certain approximations. Even when this does not fully apply, analysis of the MSE budget can guide hypotheses regarding mechanism. An effective static stability for deep convective motions, the gross moist stability (sections 10.2.3), also arises under certain conditions, and greatly simplifies understanding of phenomena to which it applies. In presenting these, it has proved tempting to include comments regarding extensions or ongoing work (sections 10.2.2 and 10.2.4) that are aimed at those familiar with this area.

10.2.1 Moist static energy budget

The vertically integrated thermodynamic equation and moisture equation from the primitive equations are

$$\partial_t \langle T \rangle + \langle \mathbf{v} \cdot \nabla T \rangle + \langle \omega \partial_p s \rangle = \langle Q_c \rangle + S^{\text{net}} + R^{\text{net}} + H \quad (10.1)$$

$$\partial_t \langle q \rangle + \langle \mathbf{v} \cdot \nabla q \rangle + \langle \omega \partial_p q \rangle = \langle Q_q \rangle + E. \quad (10.2)$$

where the pressure p is used as the vertical coordinate. The dry static energy is $s = T + \phi$, with ϕ the geopotential. Temperature T and specific humidity q are in J kg^{-1} , absorbing heat capacity at constant pressure and latent heat of condensation, respectively, for compactness. The sum of convective heating and moistening, Q_c and Q_q , must cancel when vertically integrated, since horizontal transport by small scale convective motions is negligible. Precipitation is given by the vertical integral of either of these terms $P = \langle Q_c \rangle = -\langle Q_q \rangle$. Vertical integrals $\langle \cdot \rangle$ through the depth of the atmosphere are here mass integrals $\int \cdot dp/g$ so all terms are in W/m^2 , following NS05.

When the vertically integrated thermodynamic equation (10.1) and moisture equation (10.2) are added, using cancellation of the convective heating and moisture sink terms, the moist static energy equation is

$$\partial_t \langle T \rangle + \langle q \rangle + \langle \mathbf{v} \cdot \nabla (T + q) \rangle + \langle \omega \partial_p h \rangle = F^{\text{net}}, \quad (10.3)$$

where the MSE is $h = s + q$.

The net flux into the atmospheric column F^{net} , signed positive when heating the atmosphere, is

$$F^{\text{net}} = F_t^{\text{net}} - F_s^{\text{net}} \quad (10.4)$$

where the net flux at the top of the atmosphere is

$$F_t^{\text{net}} = S_t^\downarrow - S_t^\uparrow - R_t^\uparrow \quad (10.5)$$

and the net surface flux, signed positive when heating the ocean, is

$$F_s^{\text{net}} = S_s^\downarrow - S_s^\uparrow + R_s^\downarrow - R_s^\uparrow - E - H. \quad (10.6)$$

Signs on individual flux terms are chosen such that they are typically positive in the climatology. Surface evaporation and sensible heat are denoted E and H . On the solar radiation terms S and longwave radiative terms R , arrows denote direction of the flux in a two-stream radiation treatment, subscripts s and t denote surface and model top and net heating of the atmospheric column terms are $S^{\text{net}} = S_t^\downarrow - S_t^\uparrow - S_s^\downarrow + S_s^\uparrow$ and $R^{\text{net}} = -R_t^\uparrow + R_s^\uparrow - R_s^\downarrow$, with $R_t^\downarrow \approx 0$.

In GCMs and in QTCM1 there are also horizontal diffusion terms in (10.3), which are small but not negligible in large-scale budgets. We omit them for presentation purposes but include them in discussion. Note that (10.3) involves neglect of time variation of surface pressure and is interpreted in the approximation that tropospheric transports dominate (or that vertical integrals are over the troposphere, with F_t^{net} at tropopause level).

10.2.2 Some remarks on format and \mathbf{v}_ψ versus \mathbf{v}_χ

Note that the $\langle \omega \partial_p \phi \rangle$ contribution to the $\langle \omega \partial_p s \rangle$ term in (10.3) is associated with conversions to the kinetic energy equation, so the MSE equation is not a standard conservation equation; h is not conserved over the domain; $\langle T + q \rangle$ is conserved by horizontal motions in absence of sources and sinks. The MSE equation is the thermodynamic contribution to the primitive equation total energy equation, in which $\langle T + q + K \rangle$ is conserved integrated over a closed domain when the kinetic energy

K equation is added. This is perhaps more clearly seen from the flux form of the MSE equation, here given for clarity in the approximation that ω terms vanish at the upper and lower limits of vertical integration. Using the continuity equation (10.8) and integration by parts, (10.3) becomes

$$\partial_t(\langle T \rangle + \langle q \rangle) + \langle \nabla \cdot (h\mathbf{v}) \rangle - \langle \mathbf{v} \cdot \nabla \phi \rangle = F^{\text{net}}. \quad (10.7)$$

The $\langle \mathbf{v} \cdot \nabla \phi \rangle$ term is the conversion to kinetic energy. The local time change term is of $\langle T + q \rangle$ but this will vanish when time averages are taken. The flux term is a flux of h , so the moist static energy equation is still appropriate, despite caveats on conservation properties.

There is a history of using a moist static energy equation that conserves h but is itself an approximation. Typically this is derived by assuming that a $-\alpha dp$ term in the thermodynamic equation can simply be replaced by $d\phi$. Because the dp is following the parcel, this assumption is inaccurate in presence of horizontal gradients. Betts (1974) gives insightful discussion of this approximate equation. The implications of using this approximation at large scales seem not to have been evaluated. The interpretation in which the MSE equation (10.3) is directly from the primitive equations but h is not conserved, is preferred here. The usefulness of (10.3) or (10.7) is due to the removal of the large but cancelling convective heating and moisture sink terms, to permit analysis of balances among terms that might seem small in the individual T and q equations but are important to the dynamics. For instance, the horizontal advection terms $\mathbf{v} \cdot \nabla(T, q)$ will prove important in some of the mechanisms discussed below.

In the horizontal advection, it can be useful to distinguish between the irrotational (purely divergent) component of the flow \mathbf{v}_χ and the nondivergent (purely rotational) component of the flow \mathbf{v}_ψ , where χ and ψ denote the associated velocity potential and streamfunction, respectively.

The continuity equation

$$\partial_p \omega = -\nabla \cdot \mathbf{v} \equiv -\nabla \cdot \mathbf{v}_\chi \quad (10.8)$$

links the vertical velocity directly to \mathbf{v}_χ . Thus this term is best conceptually combined with the vertical advection term $\langle \omega \partial_p h \rangle$. Furthermore, global conservation properties are maintained in experiments that alter the \mathbf{v}_ψ contribution since $\mathbf{v}_\psi \cdot \nabla(T + q) \equiv \nabla \cdot [\mathbf{v}_\psi(T + q)]$ vanishes in a global integral.

The properties of \mathbf{v}_ψ and \mathbf{v}_χ differ considerably in their effect on an advected scalar field, in particular moisture. The nondivergent \mathbf{v}_ψ cannot raise moisture above its upstream value. In a continent, when surface evaporation is secondary and no precipitation occurs, \mathbf{v}_ψ simply carries the inflow oceanic air mass around within the continent. On the other hand, for a field like moisture where other physics maintains a decrease of moisture with height, \mathbf{v}_χ and the implied vertical velocity acts to increase/decrease moisture when \mathbf{v}_χ is convergent/divergent at low levels.

Postulates: In GCMs, commonly $\mathbf{v} \cdot \nabla q$ and $\mathbf{v} \cdot \nabla T$ terms are not explicit but are evaluated in flux form. The following recommendations have not been tested and should be regarded as postulates.

Recommendation 1: evaluate and save the \mathbf{v}_χ and \mathbf{v}_ψ contributions of flux form transports separately in GCM runs. The MSE transport terms of (10.3) can then be

written

$$\langle \mathbf{v} \cdot \nabla(T + q) \rangle + \langle \omega \partial_p h \rangle = \langle \nabla \cdot (\mathbf{v}_\psi(T + q)) \rangle + \left[\langle \nabla \cdot (\mathbf{v}_\chi(T + q)) \rangle + \langle \omega \partial_p \phi \rangle \right]. \quad (10.9)$$

The term in square brackets relates directly to convergent motions and vertical velocity and thus with the work required to raise large scale air masses, the essence of the moist stability discussed in the following section, while the \mathbf{v}_ψ term is associated with advecting air masses horizontally without convergence. Where strong gradients occur, the term in square brackets may make more sense to interpret than ω and \mathbf{v}_χ terms separately.

Recommendation 2: In GCMs, terrain-following “sigma” coordinates are often used, but output is often interpolated to pressure levels. Sometimes variables on a staggered grid in the horizontal are also interpolated onto a common grid. The MSE budget, because of the strong cancellation between large terms, can be very sensitive to interpolation. Computing the quantities above in the native coordinates at run time and saving the vertical averages would add little to the storage requirements and much to the accuracy of MSE diagnostics.

10.2.3 Gross moist stability

Suppose for some set of phenomena of interest, associated with deep convection, one can define a dominant vertical structure of vertical velocity $\Omega_1(p)$ such that

$$\omega(x, y, p, t) \approx -\Omega_1(p) \nabla \cdot \mathbf{v}_1(x, y, t) \quad (10.10)$$

where \mathbf{v}_1 is the projection coefficient of a wind vertical structure V_1 , and

$$\Omega_1 = - \int_p^{p_s} V_1 dp. \quad (10.11)$$

Signs are chosen so that Ω_1 is positive when V_1 has the sign of upper level flow for a first baroclinic structure. One important case where this arises is given in the next section. Then the $\langle \omega \partial_p h \rangle$ term in (10.3) is replaced by

$$\langle \omega \partial_p h \rangle \approx M \nabla \cdot \mathbf{v}_1 \quad (10.12)$$

where M is the *gross moist stability* (GMS)

$$M = -\langle \Omega_1 \partial_p h \rangle \quad (10.13)$$

Here M is defined in units of J m^{-2} following NS05, i.e., absorbing (p_T/g) relative to Yu et al. (1998). This is an effective static stability for moist motions that includes the partial cancellation of adiabatic cooling by latent heating (Neelin and Held 1987; Neelin and Yu 1994).

The GMS gives a measure of the work that must be done to raise a large-scale air mass with a vertical velocity of the given vertical profile. The measure above gives the moist static energy transport by motions converging at low levels, rising and diverging aloft, under conditions where horizontal gradients are small, as is conventional to assume for dry static stability measures.

10.2.4 The gross moist stability in flux form

While the GMS has most commonly been discussed with respect to vertical motions, it applies to flux form equations as well. Integrating (10.13) by parts, and using $\Omega = 0$ at top and bottom yields

$$M = \langle V_1 h \rangle. \quad (10.14)$$

For convenience, define components of this as

$$M = M_T + M_\phi - M_q, \quad (M_T, M_\phi, M_q) = \langle V_1(T, \phi, -q) \rangle. \quad (10.15)$$

The MSE equation in flux form (10.7), assuming that limits of vertical integration have negligible gradients, that $\mathbf{v} \approx V_1(p)\mathbf{v}_1$, and taking a time average $\langle \cdot \rangle$, becomes

$$\nabla \cdot \overline{(M\mathbf{v}_1)} - \overline{\mathbf{v}_1 \cdot \nabla M_\phi} = \overline{F^{\text{net}}}. \quad (10.16)$$

where the second term, involving M_ϕ , is the conversion to kinetic energy and is presumably locally smaller than the MSE convergence, $\nabla \cdot (M\mathbf{v}_1)$. The latter can be divided into rotational and divergent components using $\mathbf{v}_1 = \mathbf{v}_{1\psi} + \mathbf{v}_{1\chi}$. The MSE convergence is then

$$\nabla \cdot (M\mathbf{v}_{1\psi}) + \nabla \cdot (M\mathbf{v}_{1\chi}) \quad (10.17)$$

with the second being due to all the effects of the divergent flow and associated vertical velocity and the first acting only by $\mathbf{v}_\psi \cdot \nabla$ advection terms.

Postulates: When strong horizontal gradients of temperature and moisture occur, then $\mathbf{v}_\chi \cdot \nabla q$ and $\mathbf{v}_\chi \cdot \nabla T$ terms can be large. The flux form of M (10.14), with (10.16), appears appropriate to these situations. In GCM diagnostics, the term in square brackets in (10.9) may provide an easier means of evaluating the MSE convergence associated with the GMS.

In defining V_1 for (10.14), it may be best to use the typical vertical structure of \mathbf{v}_χ for the region and phenomenon, since the convergent motion is so important to the energetics, but tends to be smaller than the purely rotational component. Evaluation of $V_{1\chi}(p)$ may also be aided by the tendency of $\chi = \nabla^{-2}(\nabla \cdot \mathbf{v})$ to have a smoothing effect that emphasizes larger spatial scales.

Open question: If more than one vertical structure is necessary to describe the vertical velocity field for the set of phenomena of interest, then $\langle \omega \partial_p h \rangle$ has contributions from more than one GMS (Neelin and Zeng 2000). The flux form of M makes the extension to this case appear straightforward. Using a sum of a few velocity vertical structures, $\mathbf{v} \approx \sum_i V_i(p)\mathbf{v}_i(x, y, t)$, then the MSE convergence term becomes

$$\sum_i \nabla \cdot (M_i \mathbf{v}_i), \quad \text{with } M_i = \langle V_i h \rangle. \quad (10.18)$$

Exploration of the implications of this has only recently begun, and it will be interesting to see under what conditions it leads to simple interpretation. Cases that treat slow spatial variation of Ω_1 and M may be found in Yu and Neelin (1997) and Yu et al. (1998). Moskowitz and Bretherton (2000) and Sobel and Neelin (2006) find nontrivial contributions from impacts of atmospheric boundary layer convergence

on vertical structure, bringing into a QE context effects previously noted in a large literature summarized in Chapter 8 of this volume. The likelihood that changes in vertical structures affect M in narrow ITCZs is inferred from reanalysis budgets in Back and Bretherton (2006).

10.2.5 Relationship to QE

An important case where the GMS arises is when convective QE constrains temperature (Emanuel et al. 1994) and thus baroclinic pressure gradients, and where frictional effects may be considered secondary. Then the baroclinic wind coefficient \mathbf{v}_1 appears in the divergence, giving the horizontal variations of the vertical motions, whose vertical structure has been obtained by hydrostatic and continuity constraints. A sketch of the derivation follows [for details, see Neelin (1997) and Neelin and Zeng (2000)].

Consider the momentum equations combined with the hydrostatic equation, in an approximation where friction is neglected and only the barotropic wind \mathbf{v}_0 is retained as the advecting velocity

$$(\partial_t + \mathbf{v}_0 \cdot \nabla)\mathbf{v} + f\mathbf{k} \times \mathbf{v} = -\nabla \int_p^{p_{rs}} \kappa T d \ln p - \nabla \phi_s \quad (10.19)$$

where ϕ_s is the geopotential at the surface reference pressure level, p_{rs} , and $\kappa = R/C_p$, where R is the gas constant for air, appears in the baroclinic pressure gradient term since T has absorbed C_p .

If QE tends to move the column toward a preferred temperature structure such that

$$\nabla T \approx a_1(p) \nabla T_1(x, y, t), \quad (10.20)$$

then (10.19) can be separated to yield an equation for the barotropic velocity component \mathbf{v}_0 with constant vertical structure and an equation for a baroclinic velocity component \mathbf{v}_1 driven by the baroclinic pressure gradients associated with T_1 . The associated baroclinic vertical structure

$$V_1(p) = a_1^+ - \widehat{a_1^+} \quad (10.21)$$

where $a_1^+ = \int_p^{p_{rs}} \kappa a_1 d \ln p$. From (10.21), $\Omega_1(p)$ can be derived by the continuity equation (10.11). The gross moist stability (10.13), then arises naturally for motions obeying QE.

Open questions: This derivation will not work uniformly for all motions. At small scales, departures from QE temperature structure will occur. Yu and Neelin (1994) have noted that QE slowly gives way to other balances as one moves from large spatial scales to scales much smaller than the time scale on which convection establishes QE times the gravity wave speed. In other situations, baroclinic pressure gradients may not dominate friction or baroclinic advection. For instance, Back and Bretherton (2006) have noted that in the zonally elongated intertropical convection zones (ITCZs), MSE balances occur in which $\omega \partial_p h$ is not the dominant export of MSE, and strong low-level convergence occurs.

Postulate: In ITCZs the meridional velocity is primarily balanced by friction at low levels and baroclinic advection at upper levels, not by meridional pressure

gradients. The vertical structure of the mean meridional wind is then not given by (10.21). However, a large-scale wave disturbance passing through the same ITCZ whose convergent velocity does obey these balances will experience a QE-based GMS.

10.3 QTCM

The QTCM, introduced in Neelin and Zeng (2000) and Zeng et al. (2000) projects the primitive equations onto vertical basis functions that are derived under QE approximations as in the previous sections. The resulting equations are not necessarily in or near QE unless convection happens to be very strong at a particular location, but the vertical structures are well suited to QE conditions.

The MSE budget for QTCM1 is a close counterpart to the primitive equations case (10.3). The considerations of the previous section lead to the simpler form for the MSE divergence term (10.12) with M given by (10.13).

Here the anomaly case is presented for use in discussion of teleconnection or global warming anomalies. For time averages over some period of interest \bar{X}^t as departure from a climatology \bar{X}^c , the anomaly is $X' = \bar{X}^t - \bar{X}^c$. Neglecting time derivative terms, the anomaly MSE equation becomes

$$(M\nabla \cdot \mathbf{v}_1)' + \langle \mathbf{v} \cdot \nabla T \rangle' + \langle \mathbf{v} \cdot \nabla q \rangle' = F_t^{\text{net}'} - F_s^{\text{net}'} \quad (10.22)$$

where the vertical integrals are evaluated on the retained vertical structures. The time averages can also be extended to include ensemble averaging from a set of numerical experiments. Anomalies in nonlinear terms such as $\langle \mathbf{v} \cdot \nabla q \rangle'$ contain changes in the contributions of transients. For instance, if double primes denote departures from the time average in which they occur (\bar{X}^t or \bar{X}^c), there are transient terms such as $\langle \omega'' \partial_p h'' \rangle'$ as discussed in Su and Neelin (2002). The transient term will be carried, although discussion will center on terms like $\bar{M} \nabla \cdot \mathbf{v}_1'$.

Postulate: The role of terms due to transients is likely to be scale dependent, since at the scale of individual convective elements, transients must dominate. Evaluation of (10.9) with some spatial averaging scale may be a route to resolving this. While the transient terms can be important in the climatology, for climate anomalies their role is not clear. In QTCM simulations (which have substantial explicit diffusion presumed to stand in for some aspects of transients), the role of transients is often, though not always, secondary. This appears not to have been well examined in observations.

10.4 SOME IMPLICATIONS OF THE MSE BUDGET AND QE

10.4.1 Implications for land convective zones

Because of the low heat capacity over land, the net surface energy flux on time scales longer than a day obeys

$$F_s^{\text{net}} = 0 \quad (10.23)$$

so F_s^{net} drops out of (10.3) over land. Under conditions where the MSE budget is the leading thermodynamic balance this provides considerable simplifications for treatment of land surface feedbacks within convection zones (Zeng and Neelin 1999; Neelin and Zeng 2000). Only top-of-atmosphere radiative forcing F_t^{net} and transport processes, i.e., advection of temperature and moisture, come into play in balancing the MSE divergence.

To a first approximation, i.e., to the extent that convective QE holds and the MSE budget alone controls the dynamics in the convective zones, the atmospheric dynamics can be solved without any reference to T'_s . The partition between E' and other fluxes does have some effect, especially when departures from QE must be considered. Nonetheless, this is a powerful leading order simplification. The physics can be understood as follows: in a deep convective region, moisture and temperature equations are being strongly linked by convection through the entire troposphere; the partition between latent and other forms of heat release at the surface is thus less important at leading order than the flux of all forms of energy into the tropospheric column.

10.4.2 Land-ocean contrast and the net flux into the atmosphere

The consequences of the zero net flux condition (10.23) over land for land-ocean contrast are striking. Figure 10.4 shows an estimate of the net flux into the atmospheric column from observations (Chou and Neelin 2001; CN03). The top-of-atmosphere net flux is from the Earth Radiation Budget Experiment. Over land, this is the only flux required, due to (10.23). Over ocean there is a strong net surface flux varying with season, balanced by ocean heat storage and transport. While estimates of the net flux at the ocean surface differ in detail among data sets [here from the Comprehensive Ocean-Atmosphere Data Set and Darnell et al. (1992) shortwave], the land-ocean contrast is large enough to be a robust feature. Seasonally, at midlatitudes it is on the order of 50-100 W/m² difference from land to ocean. In the tropics, differences between ocean regions with large heat export and continents have similar magnitude. In the view argued here, this difference in net flux is the leading cause of land-ocean contrast, not surface temperature. Consequences of this difference for summer monsoons are elaborated in the following section.

10.5 DYNAMICAL MECHANISMS IN MONSOON POLEWARD BOUNDARIES

Comparing the poleward boundary of strong seasonal precipitation in Fig. 10.1c,d with the poleward extent of positive net flux into the atmospheric column over summer continents in Fig. 10.4 raises a question posed in Chou et al. (2001), Chou and Neelin (2001) and CN03. If the leading balance typical of tropical dynamics applied, positive net flux into the column would lead to rising motion and precipitation, with the associated low-level convergence supplying sufficient moisture to meet the convective threshold (a substantial fraction of the time). Since the bound-

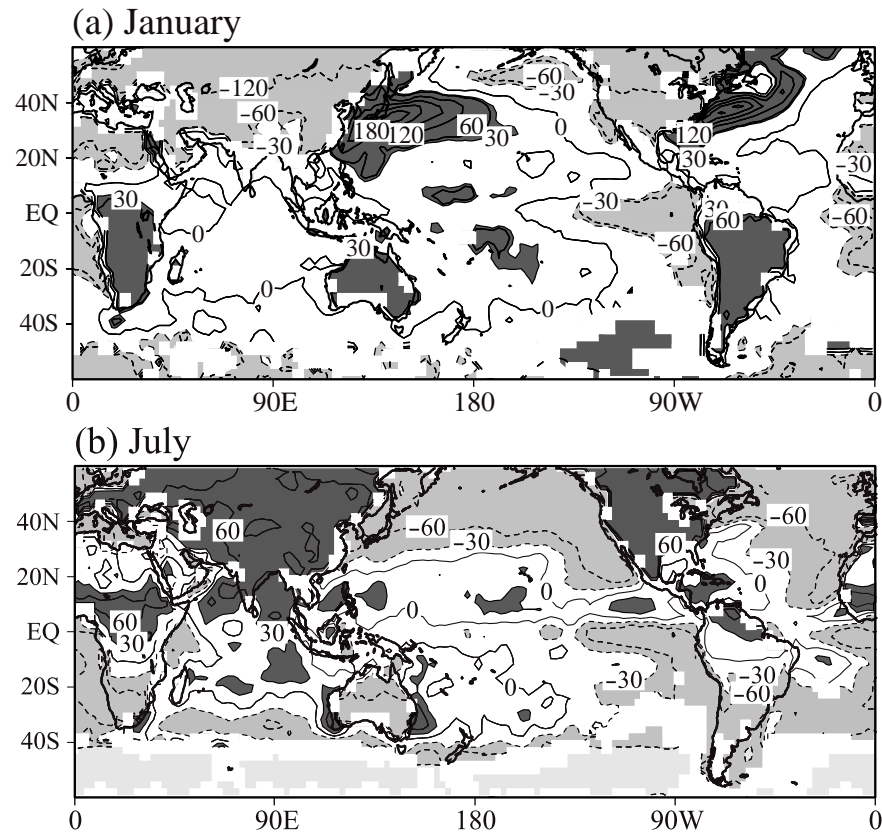


Figure 10.4 Net flux into the atmospheric column of longwave, shortwave, sensible and latent heat through surface and top of the atmosphere, estimated from observations for (a) January (from Chou and Neelin 2001) and (b) July (from Chou and Neelin 2003).

ary of the convection zone, as measured by substantial precipitation, clearly does not extend nearly as far poleward as the region of positive net flux, there must be a transition in terms of the dynamics of the system that sets this boundary. What are the dynamics setting the poleward boundary?

Two main dynamics mechanisms were found.

(i) The ventilation mechanism, defined as the import into the continents of low moist static energy air from ocean regions (or export of high moist static energy from continents). Advection terms $\mathbf{v}_\psi(T + q)$ are important to this import, which breaks the simplest balance introduced above, and prevents convective criteria from being reached in large parts of the continent. Ocean seasonal heat storage and transport keep the oceanic MSE low relative to what would be required to meet convective criteria in a warm continent.

(ii) The “interactive Rodwell-Hoskins” (IRH) mechanism due interaction of Rossby-

wave-induced subsidence to the west of monsoon heating with the convergence zone. Rodwell and Hoskins (1996; 2001) examined baroclinic Rossby wave subsidence to the west of a specified heating. The adjective “interactive” in IRH is intended to underline that the monsoon heating and its spatial pattern are themselves determined interactively with the subsidence pattern.

To test the ventilation mechanism, CN03 suppressed the $\mathbf{v}_\psi \cdot \nabla(q, T)$ terms in the model moisture and temperature equation over target regions. Note that conservation relations are maintained within the target region since \mathbf{v}_ψ is divergenceless (see section 10.2.1 or CN03 for details). They found that when ventilation is suppressed, monsoon rainfall indeed extends far poleward of the normal boundary for North American and Asian monsoons, while similar experiments in Chou and Neelin (2001) showed the same for the South American case. The exception is the northern African summer monsoon, where albedo plays a lead role in current climatology. This may be anticipated from Fig. 10.4 since over northern Africa, there is not a substantial net flux of energy into the atmospheric column. In the model, if albedo is artificially set to constant over northern Africa, then the dynamical mechanisms become important. Implications of the ventilation mechanism for the mid-Holocene “green Sahara” problem are explored in Su and Neelin (2005) and Hales et al. (2006) including interaction with vegetation feedback.

An example of the effects of the ventilation mechanism is seen in Fig. 10.5. Rather than showing climatologies with and without ventilation, it shows a succession of days during the transition from an experiment with ventilation suppressed to an experiment with standard model dynamics. The initial and final contour roughly typify the climatology without and with ventilation, respectively. There is transient synoptic variability present as well, but the change over the continent is representative of the change in the climatology (CN03). The 2 mm/day precipitation contour is used as a measure of the edge of the convection zone (monsoon boundary). In the climatology, the model maximum precipitation over Mexico reaches 10 mm/day.

While the ventilation is off, the precipitation extends far poleward over the continent. A dry region persists in the southwestern U.S. due to the IRH mechanism. In general both ventilation and IRH mechanisms contribute to east-west asymmetry in the continent and maintenance of southwestern deserts. Suppressing the beta effect has been used to demonstrate the role of IRH internal Rossby wave dynamics in this.

When the ventilation is restored, the oceanic air mass sweeps into the continent over a period of a week, carrying modest moisture values insufficient to maintain sustained convection over most of the continent.

Open questions: such experiments have not been conducted on full general circulation models, so there is as yet no corroboration of the mechanisms analysed in the QTCM. Analysis of output might yield some insight, although challenges exist because of the number of features acting at once. For instance, an oceanic air mass carried into a dry region created by subsidence tends to raise moisture, but when carried into a region that has enough moisture to meet convective criteria over a warm continent it tends to reduce moisture.

Postulate: A potentially useful (but untested) diagnostic: find the low-level moisture or moist static energy value that would be required to initiate convection at

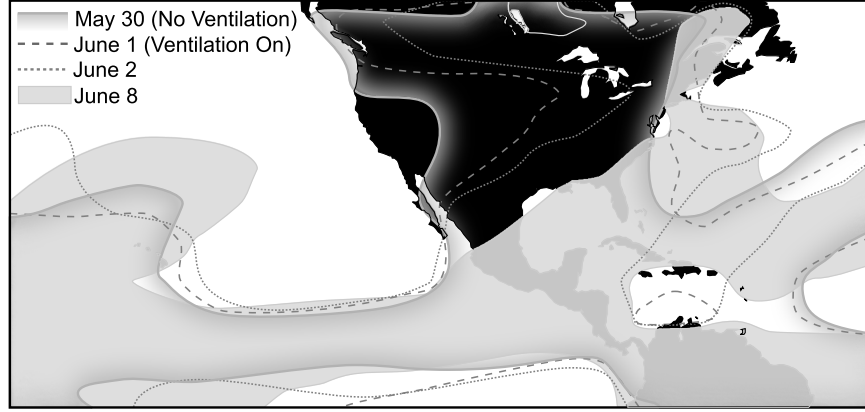


Figure 10.5 Boundary of the monsoon as measured by the 2 mm/day precipitation contour for an experiment where the ventilation mechanism is switched on May 30, beginning from a prior experiment where the ventilation was artificially suppressed. The precipitation thus initially extends artificially far poleward in the continent (ghost-shaded contour labelled May 30). Once the ventilation mechanism is switched on, low MSE oceanic air properties are advected in from the west. The retreat of the monsoon boundary over the subsequent week is shown by a succession of contours labelled by date. The full shaded area shows the region with precipitation exceeding 2 mm/day on June 8, which is typical of the model climatology. Data from experiments conducted for CN03.

every point in the model climatology. This would be done by approximating the value typically associated with the onset of strong convection for a given free tropospheric temperature. Tracing back along streamlines of \mathbf{v}_ψ , these values could be compared to the inflow values of moisture and potential temperature at the oceanic boundaries to address the importance of ventilation.

10.6 IMPLICATIONS OF THE MSE BUDGET AND QE: ANOMALY CASE

10.6.1 Implications for precipitation and the GMS multiplier effect

Following NS05, the moisture budget (10.2) gives the precipitation anomalies (vertically integrated convective heating) as

$$P' = (M_q \nabla \cdot \mathbf{v}_1)' - \langle \mathbf{v} \cdot \nabla q \rangle' + E' \quad (10.24)$$

Using the MSE equation (10.22) for the divergence yields

$$P' = \frac{\bar{M}_q}{M} \left[-\langle \mathbf{v} \cdot \nabla T \rangle' + F_t^{\text{net}'} - F_s^{\text{net}'} \right] - \left(\frac{\bar{M}_q}{M} + 1 \right) \langle \mathbf{v} \cdot \nabla q \rangle' + \left(-\frac{\bar{M}_q}{M} M' + M_q' \right) \nabla \cdot \bar{\mathbf{v}}_1 + E' \quad (10.25)$$

The nonlinear terms of the form $\langle \mathbf{v} \cdot \nabla q \rangle'$ must be expanded into \mathbf{v}' and q' contributions (and an additional term for changes in transients). Each term in (10.25)

is typically associated with some particular pathway for precipitation anomaly impacts, as elaborated in sections 10.9 and 10.10.

The factor (\bar{M}_q/\bar{M}) is a measure of the moisture convergence relative to the MSE divergence. This factor tends to be several times larger than unity (Yu et al. 1998, Zeng and Neelin 1999). NS05 refer to the effects summarized in (M_q/M) as the *GMS multiplier effect*. It boosts a small signal in the MSE equation to a convective heating and precipitation impact several times larger. This effect is basically what has earlier been referred to as a “convergence feedback” (Webster 1972; Zebiak 1986) recast in terms of moist thermodynamics. In the observation-based estimates of Yu et al. (1998), this would be roughly 4 or 5 in the deep convective zones.

Postulate: Even for GCMs where M has not been estimated or where it is challenging to do so, the principle of this effect may be evaluated: that large vertical velocity and moisture convergence, with large consequences for precipitation, may occur with little work being done in the MSE equation.

10.6.2 Implications for anomalies over ocean

Consider an ocean surface layer governed by

$$\partial_t(c_s T_s)' + D_s' = F_s^{\text{net}'} \quad (10.26)$$

where T_s is SST and we have assumed the vertical integral over the ocean surface layer $\int_s \rho c_w T' dz \approx c_s T_s'$ so c_s is an effective heat capacity of the layer; D_s is the divergence of the ocean heat transport in the layer, including turbulent and advective fluxes from below; and primes denote anomalies. A simple case is a passive ocean surface layer, such as a fixed-depth mixed layer, simply reacting to atmospheric heat flux anomalies with $D_s' = 0$. The surface layer energy budget (10.26) then implies that surface flux vanishes when the layer equilibrates and $c_s \partial_t T_s' \rightarrow 0$. Thus despite non-zero SST anomalies, the $F_s^{\text{net}'}$ term drops out of the perturbation MSE budget (10.22) and hence out of the precipitation anomaly equation (10.25). While the ocean is in disequilibrium with the teleconnected forcing, the SST anomaly can contribute to driving MSE divergence. Once the SST anomaly reaches approximate equilibrium with the atmosphere, then the SST is approximately a by-product in convective regions, much like the land surface temperature. This has considerable implications for global warming cases, where near-equilibrium conditions often apply. For regions where net surface flux is small compared with other terms in the anomaly MSE budget, the SST anomaly should be regarded as a by-product in analysing precipitation changes.

Open questions: To what extent do disequilibrium surface fluxes contribute to precipitation anomalies in interannual teleconnections? If anomalies in winds or surface fluxes create changes in ocean transports, then the conditions above do not hold. Non-zero net surface flux can then continue to impact the atmospheric MSE budget and drive sustained anomalies. For which phenomena is this important?

10.7 CLOUD-RADIATIVE FEEDBACKS AS A MODIFICATION TO THE EFFECTIVE STATIC STABILITY

A manipulation of cloud-radiative effects that clarifies their nature as a feedback was presented in Zeng and Neelin (1999) for the land case (under different notation) and in Su and Neelin (2002) for the ocean case. Here, these cases are summarized and contrasted under uniform notation following NS05. Versions have been used in Bretherton and Sobel (2002), and Sobel and Gildor (2003).

Both solar and longwave feedbacks involving deep clouds and the associated cirrostratus/cirrocumulus (CsCc) have a strong linkage to convection and thus to precipitation. For land regions, only the top-of-atmosphere radiative fluxes count in the MSE budget, while over the ocean, in presence of non-zero net surface flux, the net forcing at top-of-atmosphere minus surface is important. The cloud-radiative forcing (CRF) at top-of-atmosphere, CRF_t' , and the net cloud radiative forcing on the tropospheric column $CRF^{\text{net}'}$ can be approximated as feedback terms proportional to precipitation,

$$\begin{aligned} CRF_t' &\approx C_t P', & \text{land} \\ CRF^{\text{net}'} &\approx C_{\text{net}} P', & \text{ocean.} \end{aligned} \quad (10.27)$$

The coefficients of these linearizations depend on basic state and thus on location; for instance, mean cloudiness and surface albedo are important to the shortwave contribution. For the parameters in QTCM v2.2, for example, over equatorial South America $C_t \approx -0.05$, and over the equatorial Atlantic $C_{\text{net}} \approx 0.12$. Positive C_{net} indicates CRF tending to warm the atmospheric column where there is a positive precipitation anomaly, while the small negative C_t corresponds to deep cloud feedbacks tending to slightly cool the whole column including the surface when the latter is equilibrated. Because C_t results from cancellation of large individual longwave and shortwave terms, it is smaller and more sensitive than C_{net} . The value that applies over ocean on short-time scales, C_{net} , is larger because surface fluxes are lost (at least temporarily) into the ocean. Longwave heating of the column with increased cloud dominates this term.

An approximate MSE budget that takes the CRF into account can thus be written [using the moisture equation (10.2) to rewrite P' in (10.27) as moisture convergence and other terms] as

$$(M_{\text{eff}} \nabla \cdot \mathbf{v}_1)' + \langle \mathbf{v} \cdot \nabla T \rangle' + (1 + C) \langle \mathbf{v} \cdot \nabla q \rangle' = F_{\text{eff}}^{\text{net}'} \quad (10.28)$$

where an effective moist stability M_{eff} that includes cloud-radiative feedbacks has been defined as

$$M_{\text{eff}} = M - M_{\text{CRF}} = M - C M_q, \quad (10.29)$$

$$C = C_t, \text{ land; or } C = C_{\text{net}}, \text{ ocean.} \quad (10.30)$$

The effective flux forcing occurring in tropospheric MSE budget is approximately (neglecting nonlinear cross terms, notably between cloud and moisture effects)

$$\begin{aligned} F_{\text{eff}}^{\text{net}'} &= \epsilon_{Tt} T_1' + \epsilon_{qt} q_1' + \epsilon_{T_s t} T_s', & \text{land} \\ &= \epsilon_T T_1' + \epsilon_q q_1' + \epsilon_{T_s} T_s' + (1+C) E' + H' & \text{ocean} \end{aligned} \quad (10.31)$$

where $\epsilon_T = \epsilon_{T_t} + \epsilon_{T_s}$ is the longwave cooling rate of the troposphere per unit temperature, given by top-of-atmosphere and surface contributions ϵ_{T_t} , ϵ_{T_s} and similarly for moisture longwave coefficients $\epsilon_q = \epsilon_{q_t} + \epsilon_{q_s}$; ϵ_{T_s} is the coefficient for tropospheric absorption of longwave radiation due to surface temperature anomalies T'_s ; $\epsilon_{T_s t}$ is the (small) coefficient of top-of-atmosphere contribution of T'_s to OLR; and T_1 , q_1 are projections of temperature and moisture on their respective typical vertical profiles (Zeng et al. 2000).

When evaporation is linearized, and QE is applied to link q' to T' (and land surface feedbacks are incorporated in the land case), this effective flux has the form

$$F_{\text{eff}}^{\text{net}'} = \epsilon_{\text{eff}}^{\text{net}} T'_1 \quad (10.32)$$

where $\epsilon_{\text{eff}}^{\text{net}}$ changes from land to ocean, being roughly twice as large over oceans due to downward loss to the surface, while over land there is only loss to space due to the zero net surface flux condition.

In summary, the zero net surface flux condition over land allows land surface feedbacks and cloud-radiative feedbacks to be combined into a modification of the GMS. This modification is small over land due to approximate cancellation of longwave and shortwave feedbacks. Over oceans, on time scales shorter than equilibration of the ocean surface layer, the effective moist stability can be reduced by more than 25% due to cloud longwave feedbacks. This can enhance vertical velocity anomalies and thus precipitation anomalies.

10.8 KELVINOID SOLUTION AS AN EXAMPLE OF MOIST WAVE DYNAMICS

The remote impacts, for instance, of ENSO Pacific SST variations must be mediated by wave dynamics, and tropospheric temperature is a good indicator of the baroclinic contribution to this. Figure 10.6 presents the ENSO composite corresponding to Figure 10.2 but for vertically averaged temperature above the boundary layer. A reanalysis product (which should be reliable proxy for observations since satellite tropospheric temperature estimates are assimilated) and the same three models are shown. The comparison between models and observations is considerably better than in precipitation, at least in terms of the general features of the tropical warming signal, and the models agree reasonably well over the equatorial Pacific and South America.

Among the qualitative features are that warming is confined within on the order of 20 degrees of latitude of the equator, maxima just off the equator in the Pacific consistent with Rossby wave dynamics, and an equatorial eastward extension of the warming that one might hypothesize to be in some way related to Kelvin wave dynamics, albeit with some more complicated features that vary among models. If the pattern over Africa is related to this eastward extension, then there is a poorly explained increase relative to the Atlantic. In both observations and models, there is a substantial gradient of temperature both westward of the main ENSO region and in the eastward warming over South America. This gradient changes as a function of lag (e.g., Chiang and Sobel 2002).

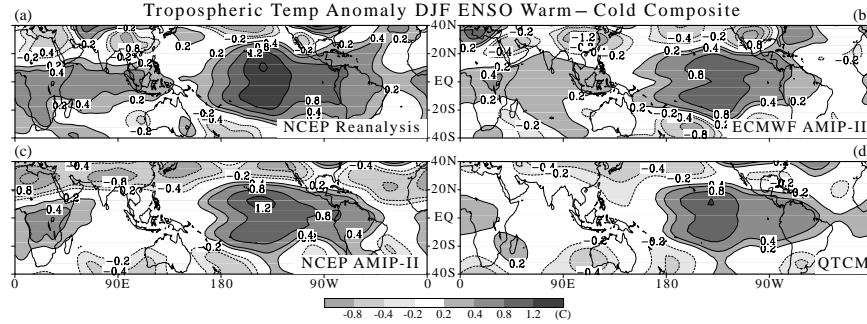


Figure 10.6 Composite tropospheric temperature anomaly (200-850 mb average) (C) for ENSO events during DJF. (a) NCEP Reanalysis (assimilated observations) and three models forced by observed SST as in Fig. 10.2. (b) ECMWF model; (c) NCEP model; (d) QTCM v2.3.

To provide an example of how such gradients might be affected by moist dynamics, the “Kelvinoid” solution of NS05 is useful. They include momentum damping but the simplest instance occurs when this is neglected.

A simple case of the momentum equation for baroclinic mode zonal wind anomalies u'_1 has the form

$$\partial_t u'_1 + \bar{u}_u \partial_x u'_1 + \kappa \partial_x T'_1 = 0 \quad (10.33)$$

for a solution with negligible v' and damping, where \bar{u}_u is a suitable projection of the mean wind, assumed constant. In steady state, the balance in (10.33) is between momentum advection and the baroclinic pressure gradient term resulting in a relationship (for $\partial_x(u, T) \neq 0$) $(-\bar{u}_u)u'_1 = \kappa T'_1$ between anomalies of wind and temperature that depends on the mean wind. Geostrophic balance of u'_1 with $\partial_y T'_1$ immediately yields Gaussian y -dependence with length scale $[(-\bar{u}_u)/\beta]^{1/2}$. While this is the same as a stationary Rossby wave scale, the balances here differ; it is simply the only available scale since the y -structure can be obtained from the vorticity equation alone with no reference to the x -structure. In more general cases, for instance if a term representing surface drag/convective momentum transport is included, the radius of deformation also enters.

Combining steady (10.33) with a similar form of (10.28) and using the QE temperature-moisture relation yields a moist wave equation of the form

$$(c_{\text{eff}}^2 - \bar{u}_u \bar{u}_h) \partial_x T'_1 = \bar{u}_u \epsilon_{\text{eff}}^{\text{net}} T'_1 \quad (10.34)$$

where c_{eff} is an effective moist phase speed (see also Chapter 7 of this volume) that is proportional to $M_{\text{eff}}^{1/2}$; \bar{u}_h is the mean wind with a vertical projection suitable to the MSE equation (10.28).

The solution decays eastward at a rate that depends on \bar{u}_u , c_{eff}^2 and $\epsilon_{\text{eff}}^{\text{net}}$. Compared to land, ocean regions have smaller c_{eff}^2 due to cloud feedbacks (10.29), and larger $\epsilon_{\text{eff}}^{\text{net}}$ (10.32) due to surface fluxes. This switch in the parameters of (10.34) creates changes in divergence, vertical velocity and precipitation just associated with land-ocean contrast. Furthermore, the $\mathbf{v} \cdot \nabla(T + q)$ terms of (10.28) give

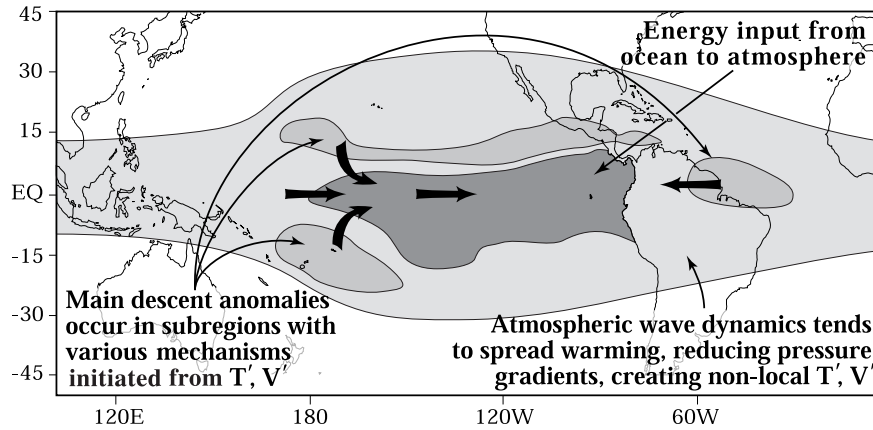


Figure 10.7 Schematic modified from Su and Neelin (2002) of a basic principle postulated to occur in moist teleconnections, here shown for the case of a warm ENSO event in the Pacific. Wave dynamics acting to reduce baroclinic pressure gradients spreads the warming from the Pacific. The teleconnected warming and associated circulation anomalies then interact with convection in a manner that depends on basic state circulation, moisture, temperature and convective thresholds. In particular subregions, conditions are satisfied for strong local descent and precipitation anomalies. A number of moist thermodynamic balances can apply in these regions, as elaborated in Table 1.

rise to the \bar{u}_h term of (10.34). It may be seen that the gradient of temperature and thus divergence depends on the interplay of these with the work done against the effective moist stability. This can be interpreted as the basic state velocity opposing effects associated with an eastward phase speed, permitting the flux terms to have more effect per unit distance.

Postulates: inclusion of varying basic state in (10.33) has impacts in addition to the basic state variations discussed above. Ongoing work to quantify this may help shed light on the temperature variations seen in Fig. 10.6. The wave equation (10.34) does not include moisture gradients due to exit from convection zones, essential to one mechanism discussed below that applies on margins of convection zones. Extensions to this case are feasible.

10.9 MOIST TELECONNECTION MECHANISMS

As summarized in section 10.1.3, teleconnections in the tropics—including the important impacts on land precipitation—are complicated by interactions with convective heating, shortwave and longwave cloud-radiative feedbacks and land-surface feedbacks. Traditional notions of descent anomalies being balanced by radiative cooling, such as are implicit in Gill (1980), are argued here and in Su and Neelin (2002) and NS05 not to be leading balances in the regions of strongest precipitation and descent anomalies. Using the MSE budget and QE considerations outlined

above aids understanding of the contributing mechanisms.

The main principles common to all mechanisms are schematized in Fig. 10.7, adapted from Su and Neelin (2002).

(i) *Wave dynamics* acts to reduce baroclinic pressure gradients that would otherwise be created by the local heating by surface fluxes in the source region (e.g., during El Niño), spreading warm temperatures.

(ii) The direct effects of the wave dynamics are expressed by tropospheric temperature anomalies T' and by the associated wind anomalies \mathbf{v}' . Convective QE links moisture anomalies q' to T' within convection zones (QE mediation). The teleconnected T' , \mathbf{v}' and the QE-mediated q' impact various terms in the MSE budget in particular regions determined by basic state conditions.

(iii) Anomalies in the vertical motion determined by interplay with other terms in the MSE equation imply large effects on precipitation since anomalous moisture convergence tends to be much larger than the associated MSE divergence (the GMS multiplier effect of section 10.6.1).

In analyzing these teleconnections, we have simplifications outlined in previous sections, which hold under specified approximations, from (i) The GMS, M (section 10.2.3), which accounts for the partial cancellation of adiabatic cooling by convective heating as a reduced static stability; (ii) the zero net surface flux condition over land (section 10.4.1) within convecting regions (where moisture equation and dry thermodynamic equation are linked by convection); (iii) cloud-radiative feedbacks as a change in M (section 10.7). These simplifications help to handle some of the feedbacks, while analysis of the MSE budget shows which terms balance anomalous descent.

This yields a small “zoo” of mechanisms, summarized in Table 1, many of which have overlapping steps in their pathways. Mechanisms are stated here for an El Niño warming case but the mechanisms also tend to work for a La Niña case with signs reversed, e.g., cool troposphere is in QE with reduced low-level moisture. These can be tested numerically in experiments that artificially suppress terms involved in the mechanism. Different mechanisms hold in particular subregions within the area where wave dynamics has affected tropospheric temperature, wind and moisture. Note that the mechanisms are not additive and some have common elements. Regarding terminology, C. Bretherton has suggested that “effect” might sound better than “mechanism”. Definitions—respectively, “effect [...] a real phenomenon, usually named after its discoverer”, and “mechanism [...] the means by which an effect is produced” (per Webster’s dictionary)—allow for either. Here the term originally appearing in the literature is used for simplicity and readers may substitute “effect”, as in “upped-ante effect”, if they prefer.

10.9.1 The upped-ante mechanism

Figure 10.8 shows a schematic of the upped-ante mechanisms. In convective regions, an increase in tropospheric temperature would tend to decrease parcel buoyancy unless low level moist static energy increases to compensate. In NCS03 terminology motivated by a poker analogy, this “ups the ante” for the amount of lower tropospheric moisture a region must have to convect, in competition with neighbor-

Table 10.1 Moist teleconnection mechanisms, with emphasis on those leading to precipitation anomalies. Note that not all are independent. “Common” denotes effects common to several or all mechanisms. Right arrows indicate causal pathways between mnemonic symbols indicating the terms involved. The gross moist stability (GMS) is M , \mathbf{v} is horizontal velocity, $\nabla \cdot \mathbf{v}'$ is a measure of the divergence and vertical velocity anomaly, T' is free tropospheric temperature anomaly, q' is low-level moisture anomaly; c_{eff}^2 is proportional to M_{eff} and measures wave propagation propagation relative to mean flow projections \bar{u}_h, \bar{u}_u ; $F_s^{\text{net}'}$ is net surface flux anomaly, S_s' is net surface shortwave anomaly and T_s is SST.

Mechanism	Pathway or Mediating Term
GMS multiplier effect (common)	MSE equation $\Rightarrow \nabla \cdot \mathbf{v}' \Rightarrow P' \approx (M_q/M)\nabla \cdot \mathbf{v}'$
QE mediation (common)	Convection links low-level q' with free tropospheric T'
Cloud-radiative feedback (common)	CRF $\approx M_{\text{CRF}}\nabla \cdot \mathbf{v}'$ acts like modification to GMS; $M_{\text{eff}} = (M - M_{\text{CRF}})$ differs between land and ocean
Upped-ante mechanism	Teleconnected $T' \Rightarrow q' \Rightarrow \bar{\mathbf{v}} \cdot \nabla q'$
Moist wave decay mechanisms (easterly flow effects, radiative damping, surface drag)	$\mathbf{v} \cdot \nabla T'$ due to $(\mathbf{v} \cdot \nabla \mathbf{v})'$, combined with surface drag and thermal damping; e.g., $(c_{\text{eff}}^2 - \bar{u}_h \bar{u}_u)$ vs. damping
M' mechanism	$T' \Rightarrow q' \Rightarrow M'_q, M'$; $M'\nabla \cdot \bar{\mathbf{v}} \Rightarrow \bar{M}\nabla \cdot \mathbf{v}'$
Anomaly wind (\mathbf{v}') mechanisms	Teleconnected $\mathbf{v}' \Rightarrow \mathbf{v}' \cdot \nabla T, \mathbf{v}' \cdot \nabla \bar{q}, \mathbf{v}'$ effects on E'
Troposphere/SST (surface flux) disequilibrium mechanisms (CRF, QE-mediated E', \mathbf{v}' effects on E')	$T' \Rightarrow q' \Rightarrow E', \mathbf{v}' \Rightarrow E', S_s'$ yield $F_s^{\text{net}'}$ only while $\partial_t T_s' \neq 0$

ing regions for the available moisture supply. In regions where there is no other impact on the moisture or energy budget, the boundary layer moisture simply increases and precipitation continues. The moisture supply required for the increase is small and can be met by a temporary decrease in precipitation that does not persist after the moisture returns to convective QE with the warmer troposphere. However, because moisture is not being increased in neighboring non-convective regions, moisture gradients are created. In regions where there is low-level inflow of air from a non-convective region, a $\bar{\mathbf{v}} \cdot \nabla q'$ moisture advection term creates a drying effect in the margins of the convective zone. This impacts vertical motion via the GMS multiplier effect, leading to a substantial precipitation reduction from a modest $\bar{\mathbf{v}} \cdot \nabla q'$. NS05 found the upped-ante mechanism to be the leading contributor to the precipitation reduction over eastern equatorial South America and a major contributor to anomalies over the Atlantic ITCZ during ENSO.

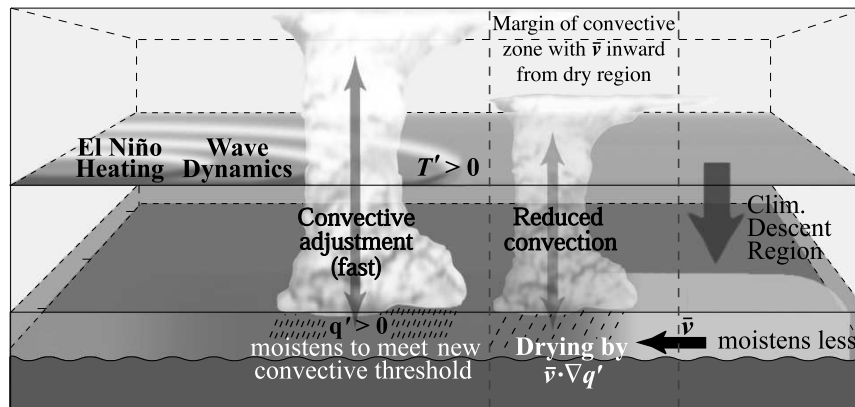


Figure 10.8 Schematic of the upped-ante mechanism. The free tropospheric temperature is affected by remote heating via wave dynamics. To maintain convection into a warmer free troposphere ($T' > 0$), the lower tropospheric moisture must increase ($q' > 0$), creating moisture gradients relative to non-convective regions. Advection by low-level inflow tends to oppose the moisture increase, leading to reduced precipitation on the margin of the convective zone. Adapted from NCS03.

10.9.2 Moist wave decay mechanisms

Section 10.8 provides an example of a moist Kelvinoid solution, a steady, eastward decaying solution that would remain after a time dependent set-up by a Kelvin wave packet interacting with moist convection, the mean flow and Rossby contributions. Some features of the interaction would also apply to decaying Rossby-wave-like solutions.

In deep convection zones, the gross moist stability implies greater vertical motion anomalies and slower phase speed than would occur for a dry wave of the same vertical structure, due to the partial cancellation of adiabatic cooling/warming by diabatic heating anomalies. The mean wind in which the wave propagates can play an important role because momentum advection terms are the main balancing for baroclinic pressure gradients; and the slow moist wave speed, on the order of 10-15 m s^{-1} , implies that the zonal wind can be comparable to the phase speed. The cancellation between \bar{u} terms, such as $\bar{u}\partial_x T'$, and the moist stability terms that give the phase speed term can increase gradients in the anomalies, i.e., faster zonal decay in T' and greater descent and precipitation anomalies. This eastward decay involved in the $\bar{u}\partial_x T'$ term can be balanced in part by radiative cooling to space, or over oceans by surface flux damping terms. Traditional notions of the balance would have suggested that radiative damping would be the leading term in driving anomalous descent. Radiative cooling associated with temperature is only a few W m^{-2} for even a large ENSO event, considerably smaller than other terms, so would not drive much descent if a dry static stability were the main balance. However, the moist processes and advection can conspire to reduce the energy required

to induce descent anomalies. Over ocean, the radiative damping effect is roughly doubled since loss occurs (temporarily) to the surface as well as to space. Surface drag communicated upward in the advection terms (as in Bacmeister and Suarez 2002), though also small, can likewise contribute to the wave decay for analogous reasons.

10.9.3 Anomaly wind mechanisms

Anomalous wind mechanisms occur via teleconnected \mathbf{v}' contributions to moisture and temperature advection, $\mathbf{v}' \cdot \nabla(\bar{q}, \bar{T})$ and to surface fluxes. The surface flux case is listed under Troposphere-SST disequilibrium mechanisms below. Su and Neelin (2002) found these are leading contributors to precipitation anomalies for ENSO impacts in the Pacific.

10.9.4 Troposphere/SST disequilibrium (surface flux) mechanisms

Mechanisms associated with surface fluxes have often been considered as a means of teleconnected warming of SST (e.g., Enfield and Mayer 1997; Klein et al. 1999; Lau and Nath 2001; Chiang and Sobel 2002). The MSE budget makes clear that the flux warming the ocean is lost from the troposphere. In deep convective regions this tends to be balanced by descent anomalies that reduce precipitation. If ocean transport divergence anomalies are negligible, then effects of surface fluxes disappear in the MSE equation once the ocean surface layer equilibrates with the troposphere. Thus SST is simply adjusted to cancel heat flux contributions by wind or tropospheric temperature plus convection—i.e., SST can be viewed as a by-product of surface heat flux equilibrium much as in the land-surface case. The proposed terminology, troposphere/SST disequilibrium, serves as a reminder that surface flux effects are temporary (unless supported by ocean heat transport) and that the free troposphere is involved as well as the atmospheric boundary layer. For the time scale of the onsetting El Niño, surface fluxes can be important. The GMS multiplier effect acts on the net surface flux anomaly to yield a substantial negative precipitation contribution.

There are several mechanisms active in producing the net surface flux anomalies. As deep convection acts to bring the boundary layer and free troposphere into QE, surface fluxes act to bring the atmospheric boundary layer and ocean surface layer into equilibrium (Chiang and Sobel 2002). Cloud-radiative feedbacks, especially shortwave, yield substantial surface warming tendency, while longwave radiative fluxes associated with temperature and moisture contribute a weaker tendency toward equilibrium with the teleconnected tropospheric warming. Additionally, teleconnections via wind create a contribution to surface flux anomalies.

10.10 MECHANISMS FOR TROPICAL REGIONAL PRECIPITATION ANOMALIES IN GLOBAL WARMING

As discussed in section 10.1.2, tropical regional precipitation anomalies simulated in global warming scenarios can be substantial. The root-mean-square change over the tropics can be significantly larger than the tropical average (Neelin et al., 2006). Three basic mechanisms have been identified based on diagnostics of the type discussed above, and in the QTCM have been verified by numerical experiments that suppress them. One mechanism is due to changes in ocean transport, which drive the atmospheric response via surface fluxes. The primary example of this occurs in the equatorial Pacific in an El Niño-like response. The other two mechanisms occur even in an equilibrated mixed-layer ocean with negligible surface fluxes. For these, SST is not useful as an indicator, since it is simply equilibrated toward a vanishing surface flux condition.

10.10.1 Upped-ante mechanism

The upped-ante mechanism in global warming works much as in the teleconnection case above (Fig. 10.8), but the tropospheric warming is due to absorption of long-wave radiation by increased greenhouse gases. The temperature equilibrates toward cancelling the top-of-atmosphere net radiative flux so there is little driving of circulation by fluxes. Instead, the large-scale warming induces differential moistening between convection zones and non-convective regions. At the inflow margins of convection zones the upped-ante mechanism then induces regional negative precipitation anomalies (NCS03, Chou and Neelin 2004). This occurs in the QTCM, and there is evidence supporting it in at least one coupled ocean-atmosphere GCM (Chou et al. 2006). The signatures to be sought in GCMs are differential moistening between convection zones and their surroundings, and regions where $\bar{\mathbf{v}} \cdot \nabla q'$ has a drying tendency coinciding with negative precipitation anomalies.

10.10.2 M' or rich-get-richer mechanism

Figure 10.9 shows a schematic of the M' (anomalous gross moist stability) mechanism, also known as the rich-get-richer mechanism since it favors precipitation increases in regions of large climatological precipitation and decreases in dry regions as the troposphere warms. Moisture increases in convective regions, as in the closely related upped-ante mechanism, to maintain QE balance with warm tropospheric temperatures. This tends to increase M_q , thus reducing M . In the anomaly MSE equation (10.22), the balance $\bar{M} \nabla \cdot \mathbf{v}'_1 = -M' \nabla \cdot \bar{\mathbf{v}}_1$, yields a low-level convergence anomaly where there is mean convergence and a low-level divergence in the climatological descent regions where $\nabla \cdot \bar{\mathbf{v}}_1$ has opposite sign. There is also a contribution by mean divergence acting on the increased moisture. Together these lead to the contribution to P' in (10.25) $(-\bar{M}_q / \bar{M} M' + M'_q) \nabla \cdot \bar{\mathbf{v}}_1$. This tends to increase precipitation in climatological convergence zones while decreasing it in subtropical descent regions. Chou and Neelin (2004) find this to be important in QTCM global warming experiments. Chou et al. (2006) find evidence in a GCM

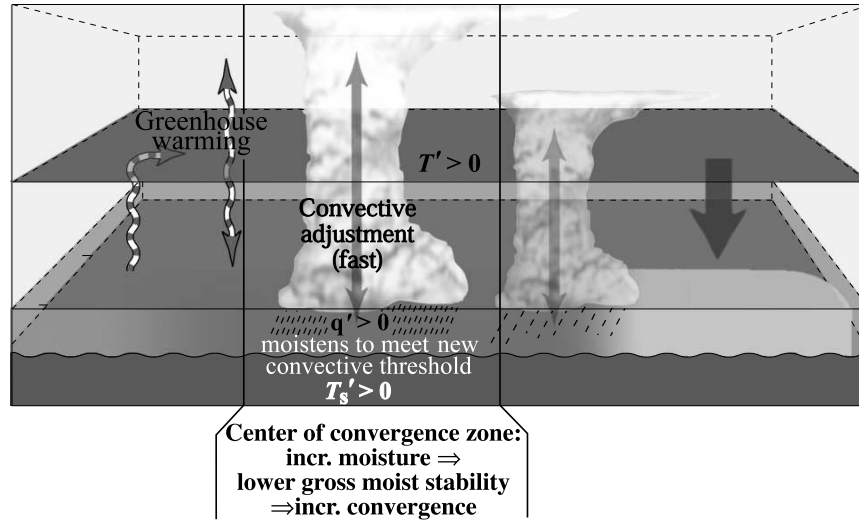


Figure 10.9 Schematic of the M' or rich-get-richer mechanism, shown for the case of tropospheric warming T' due to greenhouse gas increase. The increase of moisture with T' creates increased moisture convergence and lower gross moist stability. The latter is balanced in the moist static energy budget by additional convergence. Both aspects increase precipitation in the convergence zones and decrease it in the descent regions.

of the signature of $\langle \bar{\omega} \partial_p q' \rangle$ driving positive precipitation anomalies in the center of convection zones, enhanced by $\langle \omega' \partial_p \bar{q} \rangle$ feedback.

10.11 FINAL REMARKS.

A theme that recurs in both the ventilation mechanism, applied to the poleward extent of monsoons, and in the upped-ante mechanism, applied to precipitation changes under ENSO teleconnections and global warming, is the role of inflow of air into a region that might potentially convect. The inflow air properties must be considered relative to a critical value for convection to onset under the QE postulate, for instance, low-level moisture must exceed a threshold relative to free tropospheric temperature. Between this and the MSE and moisture budgets, the transition from convecting to non-convecting region is set (for the climatology) or shifted (for anomalies). The upped-ante mechanism and ventilation mechanisms are thus essentially variants on a theme.

The mediating terms for these mechanisms can be thought of as the advection terms, such as $\mathbf{v} \cdot \nabla q$. However, there appears likely to be an advantage to thinking in terms of advection by the purely rotational flow \mathbf{v}_ψ and the horizontally convergent flow \mathbf{v}_χ separately. The latter can be wrapped neatly with the effects of convergence/vertical velocity, including in the gross moist stability. The sum of

these effects tends to concentrate column moisture in regions of low-level convergence. The \mathbf{v}_ψ term, on the other hand, simply advects the air mass. Often the contribution of \mathbf{v}_ψ in the moisture budget is substantial, tending to oppose convection where it flows into a convection zone (in realistic cases; two-dimensional analogs, such as Hadley cell cases, typically have only \mathbf{v}_χ crossing moisture contours by construction, and thus should be used with caution). This is postulated to be implicated in the concentration of droughts in particular regions along the margins of the convective zones in global warming, and perhaps may be relevant to the sharp equatorial "notches" in the convective zones such as over Northeastern Brazil.

Theory for the gross moist stability is still at a rudimentary stage. The clearest case applies for inviscid motions when temperature structure is in convective quasi-equilibrium and the baroclinic pressure gradient is a leading term in the momentum equation. While there may be many motions in the atmosphere for which these are reasonable assumptions, there are also phenomena for which modification of these is likely required. For example, a zonally symmetric ITCZ does not have baroclinic pressure gradients balancing the convergent component of the wind, and does depend strongly on a frictional boundary layer. Zonally elongated ITCZs are then likely to require different approximations.

The approach advocated here should be viewed as one that is "in progress", with several useful results and tools, but where a number of model-based postulates must be further assessed in data, and where progress so far suggests many aspects that await refinement. It is hoped that the combination of summary and postulated directions here will help stimulate this process.

ACKNOWLEDGMENTS.

This work was supported in part by National Science Foundation grant ATM-0082529, and National Oceanographic and Atmospheric Administration grants NA05OAR4311134 and NA04OAR4310013. Graphical work by J. E. Meyerson is gratefully acknowledged. C. Chou, C. Holloway and A. Sobel provided helpful comments on the manuscript. It has been a pleasure to interact with C. Bretherton, J. Chiang, C. Chou, K. Emanuel, I. Held, B. Lintner, M. Majda, M. Munnich, A. Sobel, H. Su and others on developments in this area. Recent discussions with these and with L. Back and M. Peters have helped fuel the Open question/Postulate paragraphs.

Bibliography

- Allen, M. R. and Ingram, W. J., 2002: Constraints on future changes in climate and the hydrologic cycle. *Nature* **419**, 224–232.
- Annamalai, H.; Slingo, J.M.; Sperber, K.R.; Hodges, K., 1999: The mean evolution and variability of the Asian summer monsoon: comparison of ECMWF and NCEP-NCAR reanalyses. *Mon. Wea. Rev.*, **127**, 1157–1186.
- Arakawa, A. and W. H. Schubert, 1974: Interaction of a cumulus cloud ensemble with the large-scale environment, Part I. *J. Atmos. Sci.*, **31**, 674–701.
- Bacmeister, J. T. and M. J. Suarez, 2002: Wind Stress simulations and the equatorial momentum budget in an AGCM. *J. Atmos. Sci.*, **59**, 3051–3073.

- Back, L. E. and C. S. Bretherton, 2006: Geographic variability in the export of moist static energy and vertical motion profiles in the tropical Pacific. *Geophys. Res. Lett.*, accepted.
- Barlow, M., S. Nigam, and E. H. Berbery, 1998: Evolution of the North American monsoon system. *J. Climate*, **11**, 2238–2257.
- Betts, A. K., 1974: Further Comments on “A Comparison of the Equivalent Potential Temperature and the Static Energy”. *J. Atmos. Sci.*, **31**, 1713–1715.
- Boer, G. J., G. Flato, and D. Ramsden, 2000b: A transient climate change simulation with greenhouse gas and aerosol forcing: projected climate to the twenty-first century. *Clim. Dyn.*, **16**, 427–450.
- Bretherton, C. S. and A. H. Sobel 2002: A simple model of a convectively-coupled Walker circulation using the weak temperature gradient approximation. *J. Climate*, **15**, 2907–2920.
- Chao, W. 2000: Multiple quasi-equilibria of the ITCZ and the origin of monsoon onset. *J. Atmos. Sci.*, **52**, 641–651.
- Chiang, J. C. H., and A. H. Sobel, 2002: Tropical tropospheric temperature variations caused by ENSO and their influence on the remote tropical climate. *J. Climate*, **15**, 2616–2631.
- Chiang, J. C. H. and B. R. Lintner, 2005: Mechanisms of remote tropical surface warming during El Niño. *J. Climate*, **18**, 4130–4149, doi:10.1175/JCLI3529.1.
- Chou, C., and J. D. Neelin, 2001: Mechanisms limiting the southward extent of the South American summer monsoon. *Geophys. Res. Lett.*, **28**, 2433–2436.
- Chou, C., J. D. Neelin, and H. Su, 2001: Ocean-atmosphere-land feedbacks in an idealized monsoon, *Quart. J. Roy. Meteor. Soc.*, **127**, 1869–1891.
- Chou, C. and J. D. Neelin, 2003: Mechanisms limiting the northward extent of the northern summer monsoons over North America, Asia and Africa. *J. Climate*, **16**, 406–425.
- Chou, C. and J. D. Neelin, 2004: Mechanisms of global warming impacts on regional tropical precipitation. *J. Climate*, **17**, 2688–2701.
- Chou, C., J. D. Neelin, J.-Y. Tu, and C.-T. Chen, 2006: Regional tropical precipitation change mechanisms in ECHAM4/OPYC3 under global warming. *J. Climate*, in press.
- Cook, K. H., 1997: Large-scale atmospheric dynamics and Sahelian precipitation. *J. Climate*, **10**, 1137–1152.
- Dai, A., G. A. Meehl, W. M. Washington, T. M. L. Wigley, and J. M. Arblaster, 2001: Ensemble simulation of twenty-first century climate changes: business-as-usual versus CO₂ stabilization. *Bull. Amer. Meteor. Soc.* **82**, 2377–2388.
- Darnell, W. L., W. F. Staylor, S. K. Gupta, N. A. Ritchey and A. C. Wilber, 1992: Seasonal variation of surface radiation budget derived from international satellite cloud climatology project C1 data. *J. Geophys. Res.*, **97**, 15741–15760.
- Ding, Y.-H., 1992: Summer monsoon rainfalls in CHina. *J. Meteor. Soc. Japan*, **70**, 373–396.
- Ding, Y.-H., 1994: *Monsoons over China*. Kluwer Academic Publishers, Dordrecht. 419pp.
- Douglas, M. W., R. A. Maddox, and K. Howard, 1993: The Mexican monsoon. *J. Climate*, **6**, 1665–1678.

- Douville, H., F. Chauvin, S. Planton, J.-F. Royer, D. Salas-Méla, and S. Tyteca, 2002: Sensitivity of the hydrological cycle to increasing amounts of greenhouse gases and aerosol. *Clim. Dyn.* **20**, 45–68.
- Eltahir, E. A. B. and C. Gong, 1996: Dynamics of wet and dry years in West Africa. *J. Climate*, **9**, 1030–1042.
- Emanuel, K. A., J. D. Neelin and C. S. Bretherton, 1994: On large-scale circulations in convecting atmospheres. *Quart. J. Roy. Meteor. Soc.*, **120**, 1111–1143.
- Enfield, D. B., and D. A. Mayer, 1997: Tropical Atlantic sea surface temperature variability and its relation to El Niño-Southern Oscillation. *J. Geophys. Res.*, **102**, 929–945.
- Flohn, H., 1957: Large-scale aspects of the "summer monsoon" in south and east Asia. *J. Meteor. Soc. Japan*, **35**, 180–186.
- Gill, A. E., 1980: Some simple solutions for heat induced tropical circulation. *Quart. J. Roy. Met. Soc.*, **106**, 447–462.
- Hales, K., J. D. Neelin and N. Zeng, 2006: Interaction of vegetation and atmospheric dynamical mechanisms in the mid-Holocene African monsoon. *J. Climate*, in press.
- Higgins, R. W., Y. Yao, and X. L. Wang, 1997: Influence of the North American monsoon system on the US summer precipitation regime. *J. Climate*, **10**, 2600–2622.
- Houghton, J. T., et al., eds. 2001. *Climate Change: the scientific basis: contribution of Working Group I to the third assessment report of the Intergovernmental Panel on Climate Change Scientific Assessment*. Cambridge University Press, Cambridge, U.K.; New York. 881 pp.
- Hu, Z.-Z., M. Latif, E. Roeckner, and L. Bengtsson, 2000: Intensified Asian summer monsoon and its variability in a coupled model forced by increasing greenhouse gas concentrations. *Geophys. Res. Lett.* **27**, 2681–2684.
- Janicot, S., A. Harzallah, B. Fontaine, and V. Moron, 1998: West African monsoon dynamics and eastern equatorial Atlantic and Pacific SST anomalies (1970–88). *J. Climate*, **11**, 1874–1882.
- Johns, T. C. and coauthors, 2003: Anthropogenic climate change for 1860 to 2100 simulated with the HadCM3 model under updated emissions scenarios. *Clim. Dyn.* **20**, 583–612.
- Klein, S.A., B. J. Soden and N.-C. Lau, 1999: Remote sea surface temperature variations during ENSO: evidence for a tropical atmospheric bridge. *J. Climate*, **12**, 917–932.
- Lare, A. R. and S. E. Nicholson, 1994: Contrasting conditions of surface water balance in wet years and dry years as a possible land surface-atmosphere feedback mechanism in the West African Sahel. *J. Climate*, **7**, 653–668.
- Lau, K.-M. and S. Yang, 1996: The Asian monsoon and predictability of the tropical ocean-atmosphere system. *Quart. J. Roy. Meteor. Soc.*, **122**, 945–957.
- Lau, N.-C., and M. J. Nath, 2001: Impact of ENSO on SST variability in the north Pacific and north Atlantic: seasonal dependence and role of extratropical sea-air coupling. *J. Climate*, **14**, 2846–2866.
- Lenters, J. D. and K. H. Cook, 1997: On the origin of the Bolivian high and related circulation features of the South American climate. *J. Atmos. Sci.*, **54**, 656–677.
- Li, C. and M. Yanai, 1996: The onset and interannual variability of the Asian

- summer monsoon in relation to land-sea thermal contrast. *J. Climate*, **9**, 358–375.
- Lintner, B. R. and J. C. H. Chiang, 2005: Reorganization of tropical climate during El Niño: a weak temperature gradient approach. *J. Climate*, **18**, doi:10.1175/JCLI3580.1, 5312–5329.
- Lofgren, B. M., 1995: Surface albedo-climate feedback simulated using two-way coupling. *J. Climate*, **8**, 2543–2562.
- Luo, H. and M. Yanai, 1984: The large-scale circulation and heat sources over the Tibetan Plateau and surrounding areas during the early summer of 1979. Part II: Heat and moisture budgets. *Mon. Wea. Rev.*, **112**, 966–989.
- Manabe, S., Milly, P. C. D., and Wetherald, R., 2004: Simulated long-term changes in river discharge and soil moisture due to global warming. *Hydrolog. Sci. Jour.*, **49**, 625–642.
- Meehl, G. A., 1992: Effect of tropical topography on global climate. *Annu. Rev. Earth Planet. Sci.* **20**, 85–112.
- Meehl, G. A., 1994a: Coupled land-ocean-atmosphere processes and South Asian monsoon variability. *Science*, **266**, 263–267.
- Meehl, G. A., 1994b: Influence of the land surface in the Asian summer monsoon: External conditions versus internal feedbacks. *J. Climate*, **7**, 1033–1049.
- Meehl, G. A., W. D. Collins, B. A. Boville, J. T. Kiehl, T. M. L. Wigley, and J. M. Arblaster, 2000: Response of the NCAR climate system model to increased CO₂ and the role of physical processes. *J. Climate*, **13**, 1879–1898.
- Moskowitz B. M. and C. S. Bretherton, 2000: An Analysis of Frictional Feedback on a Moist Equatorial Kelvin Mode. *J. Atmos. Sci.*, **57**, 2188–2206.
- Murakami, T., 1987: Orography and Monsoons, in *Monsoons*, edited by J. S. Fein and P. L. Stephens, John Wiley, New York, 331–364.
- Neelin, J. D., 1997: Implications of convective quasi-equilibrium for the large-scale flow. In *The physics and parameterization of moist atmospheric convection*. R. K. Smith, ed., Kluwer Academic Publishers, Dordrecht, The Netherlands, pp. 413–446.
- Neelin, J. D., and I. M. Held, 1987: Modelling tropical convergence based on the moist static energy budget. *Mon. Wea. Rev.*, **115**, 3–12.
- Neelin, J. D., and J.-Y. Yu, 1994: Modes of tropical variability under convective adjustment and the Madden-Julian oscillation. Part I: Analytical results. *J. Atmos. Sci.*, **51**, 1876–1894.
- Neelin, J. D., and N. Zeng, 2000: A quasi-equilibrium tropical circulation model—formulation. *J. Atmos. Sci.*, **57**, 1741–1766.
- Neelin, J. D., C. Chou, and H. Su, 2003: Tropical drought regions in global warming and El Niño teleconnections. *Geophys. Res. Lett.*, **30**(24), 2275, doi:10.1029/2003GL018625.
- Neelin, J. D., and H. Su, 2005: Moist teleconnection mechanisms for the tropical South American and Atlantic sector. *J. Climate*, **18**, 3928–3950.
- Neelin, J. D., M. Munnich, H. Su, J. E. Meyerson and C. Holloway, 2006: Tropical drying trends in global warming models and observations. *Proc. Nat. Acad. Sci.*, **103**, 6110–6115.
- Nicholson, S., 2000: Land surface processes and Sahel climate. *Rev. Geophys.*, **38**, 117–139.
- Nogues-Paegle, J., C. R. Mechoso, and coauthors, 2002: Progress in Pan American

- CLIVAR Research: Understanding the South American Monsoon. *Meteorologica*, **27** 3-32.
- Palmer, T. N., 1986: Influence of the Atlantic, Pacific and Indian Oceans on Sahel rainfall. *Nature*, **322**, 251–253.
- Ramage, C. S., 1971: Monsoon Meteorology. New York: Academic. 296 pp.
- Riehl, H., 1979: Climate and Weather in the Tropics. New York: Academic. 611 pp.
- Rodwell, M. J. and B. J. Hoskins, 1996: Monsoons and the dynamics of deserts. *Quart. J. Roy. Meteor. Soc.*, **122**, 1385–1404.
- Rodwell, M. J., and B. J. Hoskins, 2001: Subtropical anticyclones and summer monsoons. *J. Climate*, **14**, 3192–3211.
- Roeckner, E., L. Bengtsson, J. Feichter, J. Lelieveld, and H. Rodhe, 1999: Transient climate change simulations with a coupled atmosphere-ocean GCM including the tropospheric sulfur cycle. *J. Clim.* **12**, 3004–3032.
- Rowell, D. P., C. K. Folland, K. Maskell and M. N. Ward, 1995: Variability of summer rainfall over tropical north Africa (1906–92): Observations and modelling. *Quart. J. Roy. Meteor. Soc.*, **121**, Part A, 669–704.
- Semazzi, F. H. M. and L. Sun, 1997: The role of orography in determining the Sahelian climate. *Int'l. J. Clim.*, **17**, 581–596.
- Sobel, A. H., and H. Gildor 2003: A simple time-dependent model of SST hot spots. *J. Climate*, **16**, 3978-3992.
- Sobel, A. H., I. M. Held, and C. S. Bretherton, 2002: The ENSO Signal in Tropical Tropospheric Temperature. *J. Climate*, **155**, 2702–2706.
- Su, H., J. D. Neelin, and C. Chou, 2001: Tropical teleconnection and local response to SST anomalies during the 1997-1998 El Niño. *J. Geophys. Res.*, **106**, D17, 20,025–20,043.
- Su, H., and J. D. Neelin, 2002: Teleconnection mechanisms for tropical Pacific descent anomalies during El Niño. *J. Atmos. Sci.*, **59**, 2694-2712.
- Sobel, A. H., and J. D. Neelin, 2006: The boundary layer contribution to intertropical convergence zones in the quasi-equilibrium tropical circulation model framework. *Theoretical and Computational Fluid Dynamics*, in press.
- Su, H., and J. D. Neelin, 2005: Dynamical mechanisms for African monsoon changes during the mid-Holocene. *J. Geophys. Res.*, **110**, D19105, doi:10.1029/2005JD005806.
- Webster, P. J., 1972: Response of the tropical atmosphere to local, steady forcing. *Mon. Wea. Rev.*, **100**, 518–541.
- Webster, P. J., 1987: The elementary monsoon, in *Monsoons*, edited by J. S. Fein and P. L. Stephens, John Wiley, New York, N.Y., 3–32.
- Webster, P. J., V. O. Magaña, T. N. Palmer, J. Shukla, R. A. Tomas, M. Yanai and T. Yasunari, 1998: Monsoons: Processes, predictability, and the prospects for prediction. *J. Geophys. Res.*, **103**, 14451-14510.
- Williams, K. D., Senior, C. A. and Mitchell, J. F. B., 2001: Transient climate change in the Hadley Centre Models: the role of physical processes. *J. Clim.* **14**, 2659–2674.
- Wu, G. and Y. Zhang, 1998: Tibetan Plateau forcing and the timing of the monsoon onset over South Asia and the South China Sea. *Mon. Wea. Rev.*, **126**, 913–927.
- Xie, P., and P. A. Arkin, 1997: Global precipitation: A 17-year monthly analy-

- sis based on gauge observations, satellite estimates, and numerical model outputs. *Bull. Amer. Meteorol. Soc.*, **78**, 2539–2558.
- Xue, Y. and J. Shukla, 1993: The influence of land surface properties on Sahel climate. Part I: Desertification. *J. Climate*, **6**, 2232–2245.
- Yanai, M. and C. Li, 1994: Mechanism of heating and the boundary layer over the Tibetan Plateau. *Mon. Wea. Rev.*, **122**, 305–323.
- Yang, S. and K.-M. Lau, 1998: Influences of sea surface temperature and ground wetness on Asian summer monsoon. *J. Climate*, **11**, 3230–3246.
- Yasunari, T. and Y. Seki, 1992: Role of Asian monsoon on the interannual variability of the global climate system. *J. Met. Soc. Japan*, **70**, 177–189.
- Yonetani, T. and H. B. Gordon, 2001: Simulated changes in the frequency of extremes and regional features of seasonal/annual temperature and precipitation when atmospheric CO₂ is doubled. *J. Clim.* **14**, 1765–1779.
- Young, J. A., 1987: Physics of monsoons: the current view, in *Monsoons*, edited by J. S. Fein and P. L. Stephens, John Wiley, New York, N.Y., 211–243.
- Yu, B. and J. M. Wallace, 2000: The principal mode of interannual variability of the North American monsoon system. *J. Climate*, **13**, 2794–2800.
- Yu, J.-Y., and J. D. Neelin, 1997: Analytic approximations for moist convectively adjusted regions. *J. Atmos. Sci.*, **54**, 1054–1063.
- Yu, J.-Y., C. Chou and J. D. Neelin, 1998: Estimating the gross moist stability of the tropical atmosphere. *J. Atmos. Sci.*, **55**, 1354–1372.
- Zebiak, S. E., 1986: Atmospheric convergence feedback in a simple model for El Niño. *Mon. Wea. Rev.*, **114**, 1263–1271.
- Zeng, N., and J. D. Neelin, 1999: A land-atmosphere interaction theory for the tropical deforestation problem. *J. Climate*, **12**, 857–872.
- Zeng, N., J. D. Neelin, and C. Chou, 2000: A quasi-equilibrium tropical circulation model—implementation and simulation. *J. Atmos. Sci.*, **57**, 1767–1796.
- Zhou, J. and K.-M. Lau, 1998: Does a monsoon climate exist over South America? *J. Climate*, **11**, 1020–1040.